the formation of a density cavity[26] (cf. profile modification) and in part by hydrodynamic expansion.

In conclusion, it has been demonstrated that resonance absorption can occur in laser-target interactions at oblique incidence. The measurements agree well with theoretical predictions for the behavior of resonance absorption and a value of 2% for the ratio of hot to cold electrons has been derived from the data. It has been shown that, with specially prepared rough surfaces, absorption can be increased, at normal incidence, probably due to resonance effects.

The authors would like to thank Professor H. P. Weber for the provision of research facilities and his interest in the work, the Swiss National Science Foundation for their funding of the work, P. Lädrach for assistance with the experiment, and J. Zimmermann, M. Coulomb, and M. Fuhrer for assistance with the laser system.

[1]R. A. Haas, W. C. Mead, W. L. Kruer, D. W. Phillion, H. N. Kornblum, J. D. Lindl, D. Mac Quigg, V. C. Rupert, and K. G. Tirsell, Phys. Fluids 20, 322 (1977).

[2]B. H. Ripin, Appl. Phys. Lett. 30, 134 (1977).

[3]E. Fabre and C. Stenz, Phys. Rev. Lett. 32, 823 (1974).

[4]J. Martineau, P. Paranthoën, M. Rabeau, and C. Patou, Opt. Commun. 15, 404 (1975).

[5]C. Yamanaka, T. Yamanaka, T. Sasaki, J. Mizui, and H. B. Kang, Phys. Rev. Lett. 32, 1038 (1974).

[6]K. Dick and H. Pepin, Opt. Commun. 13, 289 (1975).

[7]T. A. Hall and Y. Z. Negm, Opt. Commun. 16, 275 (1976).

[8]P. E. Dyer, S. A. Ramsden, J. A. Sayers, and M. A. Skipper, J. Phys. D 9, 373 (1976).

[9]T. P. Donaldson, M. Hubbard, and I. J. Spalding, Phys. Rev. Lett. 37, 1348 (1976).

[10]K. G. Estabrook, E. J. Valeo, and W. L. Kruer, Phys. Fluids 18, 1151 (1975).

[11]D. W. Forslund, J. M. Kindel, K. Lee, E. L. Lindman, and R. L. Morse, Phys. Rev. A 11, 679 (1975).

[12]M. M. Mueller, Phys. Rev. Lett. 30, 582 (1973).

[13]R. P. Godwin, Phys. Rev. Lett. 28, 85 (1972).

[14]J. L. Shohet, D. B. van Hulsteyn, S. J. Gitomer, J. F. Kephart, and R. P. Godwin, Phys. Rev. Lett. 38, 1024 (1977).

[15]J. S. Pearlman, J. J. Thomson, and C. E. Max, Phys. Rev. Lett. 38, 1397 (1977).

[16]J. S. Pearlman and M. K. Matzen, Phys. Rev. Lett. 39, 140 (1977).

[17]K. R. Manes, V. C. Rupert, J. M. Auerbach, P. Lee, and J. E. Swain, Phys. Rev. Lett. 39, 281 (1977).

[18]P. Kolodner and E. Yablonovitch, Phys. Rev. Lett. 37, 1754 (1976).

[19]W. Seka and E. Stüssi, J. Appl. Phys. 47, 3538 (1973).

[20]J. E. Balmer, T. P. Donaldson, and J. A. Zimmerman, to be published.

[21]R. B. White, C. S. Liu, and M. N. Rosenbluth, Phys. Rev. Lett. 31, 520 (1973).

[22]F. C. Jahoda, E. M. Little, W. E. Quinn, G. A. Sawyer, and T. F. Stratton, Phys. Rev 119, 843 (1960).

[23]T. P. Donaldson, to be published.

[24]J. J. Thomson, C. E. Max, J. Erkkila, and J. E. Tull, Phys. Rev. Lett. 37, 1052 (1976).

[25]T. P. Donaldson and I. J. Spalding, Phys. Rev. Lett. 36, 467 (1976).

[26]K. Estabrook, Phys. Fluids 19, 1733 (1976).

Properties of Electrostatic Ion-Cyclotron Waves in a Mirror Machine

W. C. Turner, E. J. Powers,[a] and T. C. Simonen

University of California, Lawrence Livermore Laboratory, Livermore, California 94550

(Received 10 August 1977)

Frequency and wavelength of electrostatic ion-cyclotron waves have been measured in a mirror machine. The dominant frequency occurs near the ion-cyclotron fundamental with width $\Delta f/f < 0.02$. For most of the plasma buildup and decay the perpendicular wave numbers are consistent with an ion-diamagnetic drift wave $\omega_i^* = k_\perp (cE_i/cB)(1/n)dn/dx$ at the ion-cyclotron frequency. With increasing wave amplitude the wave spectral properties do not change but an increase in ion energy diffusion is observed, supporting a wave-particle saturation of the mode.

Plasma confinement experiments in minimum-B magnetic mirror machines[1,2] have demonstrated the simultaneous reduction of hot-plasma loss rate and amplitude of ion-cyclotron oscillations with addition of warm streaming plasma injected along magnetic field lines. According to theoretical interpretation of these experiments[3] the streaming plasma stabilizes the drift cyclotron loss-cone[4] (DCLC) instability that is driven by the velocity-space loss cone of the ion distribution and the radial plasma density gradient. In this Letter we report measurements of the frequency and wavelength of the ion-cyclotron oscillations in the neutral-beam-injected 2*X*II*B* de-

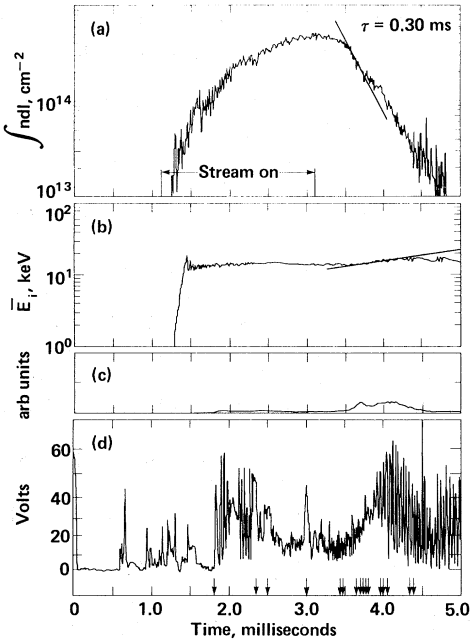

FIG. 1. Plasma measurements vs time: (a) line density, (b) mean ion energy, (c) 40-keV charge-exchange signal, and (d) amplitude of rf oscillations.

vice.[2] The vacuum field strength of the 2*XIIB* magnet is $B_{vac} = 6.4$ kg at the center and the mirror ratio $R = 2.0$. For deuterium plasmas the ion-cyclotron fundamental is 4.88 MHz at the field center.

Figure 1 shows the behavior of plasma line density, mean ion energy, envelope of rf oscillations, and 40-keV deuterium charge-exchange flux for the data to be presented. As described previously,[5] the plasma density builds up, initially by neutral (D^0) beam trapping on the stream-injected plasma, and then on the trapped hot plasma, until a quasisteady state is reached with trapped beam current matching the plasma loss rate. The stream-injected plasma source is then shut off and shortly afterward the plasma density decays with 0.30-ms decay time, although neutral beam injection continues. There is ample evidence[2,6] from plasma diamagnetism, neutron production, and energetic charge-exchange flux that the low-energy stream plasma constitutes only a small fraction of the peak density attained and that the decay is due to an increase in the hot-ion loss rate. As the density decays there is an increase in mean ion energy and a large absolute increase in the magnitude of 40-keV charge-exchange flux. This is evidence that ion energy diffusion increases when the stream plasma source is turned off. Although not observed directly, an accompanying increase of diffusion downward in energy would result in an enhanced loss current of particles reaching the ambipolar hole of the loss-cone distribution. Also shown in Fig. 1 is the amplitude of rf oscillations detected by an electrostatic probe at the edge of the plasma. The rf amplitude is high during the buildup, decreases as the peak density is reached, and then builds up again during the plasma decay. The rf amplitude occurs predominantly in a narrow band at the ion cyclotron frequency.

The ion–cyclotron-oscillation measurements were obtained with a five-tip high-impedance electostatic probe located at $z = 4$ cm from the plasma midplane at a radius $R_{probe} = 14.0$ cm. Adjacent probe separation is 1 cm. The probe tips are oriented perpendicular to field lines to measure $k_\perp$. For comparison, the mean plasma radial and longitudinal scale lengths are approximately 7 and 23 cm, respectively, and the distance between mirrors is 150 cm. Evidence that oscillations detected by the probe are driven by the hot interior plasma come from (1) agreement with the frequency of oscillation detected by a similar probe located outside the mirrors but on field lines passing through the central hot plasma; (2) agreement, at lower densities than reported here, between phase modulation frequency of a 4-mm microwave interferometer and the frequency detected by probes[7]; and (3) the observed dependence of oscillation frequency on central plasma energy density [Fig. 3(b)]. To record and analyzed the probe data we have used digital spectral analysis techniques,[8] recording the raw data on transient recorders (50-MHz digitizing rate, 2048-word, eight-bit memory), and then applying discrete Fourier analysis. Fiducial pulses are mixed with the raw data to allow corrections for time-base jitter between channels. The recorders provide a 40.96-μs time window of the plasma oscillations on a particular shot. Data have been obtained over a sequence of shots holding machine parameters constant. The transient recorder trigger times are indicated on the time axis in Fig. 1.

In Fig. 2 we have shown a typical cross-power amplitude spectrum and phase spectra. These spectra were obtained by computing the discrete Fourier transform $\Phi_j(f\alpha)$ from the time-domain data $\varphi_j(t_\beta)$ for each probe channel j using a fast Fourier-transform algorithm:

$$\Phi_j(f\alpha) = \frac{1}{N}\sum_{\beta=1}^{N} \exp(-i2\pi\alpha\beta/N)\varphi_j(t_\beta), \qquad (1)$$

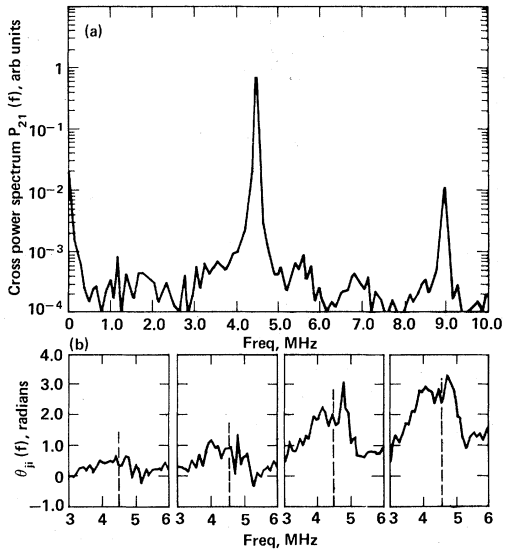

FIG. 2. (a) Cross-power amplitude spectrum $P_{21}(f)$ at $f = 4.50$ MHz. (b) Cross-power phase spectra $\theta_{21}(f)$, $\theta_{31}(f)$, $\theta_{41}(f)$, and $\theta_{51}(f)$. At $f = 4.50$ MHz, $\theta_{21} = 0.38$, $\theta_{31} = 0.84$, $\theta_{41} = 1.71$, $\theta_{51} = 2.49$, all in radians.

where $f\alpha = \alpha/N\Delta t$, $1 \leq \alpha \leq N/2$, and $t_\beta = \beta\Delta t$ with sample interval $\Delta t = 20$ ns. Cross-power spectra are then computed according to

$$P_{j1}(f\alpha) = \Phi_j^*(f\alpha)\Phi_1(f\alpha) = |P_{j1}(f\alpha)|e^{i\theta j1(f\alpha)}. \quad (2)$$

The amplitude spectrum $|P_{21}(f\alpha)|$ and phase spectra $\theta_{j1}(f\alpha) 2 \leq j \leq 5$ are plotted in Fig. 2 for a typical case. In a local plane-wave representation, the phase spectrum is related to the local wave number $k(f\alpha)$ by $\theta_{j1}(f\alpha) = k(f\alpha)\Delta x_{j1}$, where Δx_{j1} is the probe channel separation. The data in Fig. 2 have been calculated with $N = 512$ and averaging the cross-power spectrum over four segments of transient recorder memory.

The amplitude spectrum in Fig. 2 has a very narrow frequency component at $f = 4.50$ MHz near the center vacuum-field deuteron cyclotron frequency (4.88 MHz). The full width at half-maximum at 6 dB is approximately 100 kHz, and nearly equal to the width due to the finite time sample. We therefore conclude that $\Delta f/f < 0.02$ and the correlation times exceed $\sim 50/f$ (the correlation function is the Fourier transform of the cross-power spectrum). Another peak in the amplitude spectrum occurs near the first harmonic at 9.0 MHz but reduced relative to the fundamental by 18 dB. For all of the data the second harmonic is suppressed ≥ 10 dB relative to the fundamental, higher harmonics are suppressed even further, and the observed widths of the fundamental are accounted for by the finite time sample. The phase spectra in Fig. 2, evaluated at $f = 4.50$ MHz, increase with probe-tip separation. For this case, after correction for time-base jitter, a least-squares fit yields $k_\perp = 0.51 \pm 0.10$ cm^{-1} at $R_{\text{probe}} = 14$ cm. The sign of the phase shift with increasing probe separation gives the direction of wave propagation. For the conventions used, positive phase shift displayed in Fig. 2 indicates that the wave is propagating azimuthally across field lines in the direction of the ion diamagnetic drift current. Doppler-shift corrections due to plasma rotation in the ambipolar electric field are negligible. For an ambipolar potential $e\Phi \lesssim 500$ eV, corresponding to the low-energy cutoff of the ion energy distribution, we calculate the frequency of $\vec{E} \times \vec{B}$ rotation

$$f_{\vec{E}\times\vec{B}} \simeq \frac{1}{2\pi}\frac{c\Phi}{B_{\text{vac}}}\frac{1}{R_{\text{plasma}}^2} \simeq 25 \text{ kHz}.$$

In Fig. 3(a) we have summarized all of the wave-number measurements. The measurements have been scaled, assuming a radially invariant azimuthal-mode number, with the ratio of probe radius to mean plasma density radius $R_{\text{probe}}/R_{\text{plasma}} = (14 \text{ cm})/(7 \text{ cm}) = 2.0$. The data in Fig. 3(a) fall close to the condition obtained by equating the ion diamagnetic drift frequency $\omega_j^* = k_\perp(c\bar{E}_i/eB)R_{\text{plasma}}^{-1}$ to the ion cyclotron frequency which yields $k_\perp = 1.06$ cm^{-1} for $\bar{E}_i = 13$ keV, $B = 6.4$ kg, and $R_{\text{plasma}} = 7.0$ cm. The azimuthal mode number m is related to $k_\perp$ in Fig. 3(a) by $m = R_{\text{plasma}}k_\perp = 7k_\perp$. For 2.5 ms $< t <$ 4.0 ms the sign of $k_\perp$ is positive indicating waves propagating in the ion diamagnetic drift direction. These measurements of wave vector are similar to those obtained by one of us (T.C.S.) under certain operating conditions of the earlier 2*X*II experiment, which did not employ neutral beam injection or external stream stabilization. In that case the oscillations were identified as the DCLC mode.[9] Three measurements outside the interval 2.5 ms $< t <$ 4.0 ms have $k_\perp < 0$ indicating propagation in the electron diamagnetic drift direction.

The frequency of oscillation is always less than the vacuum-field cyclotron frequency. Even if the wave frequency is closely matched to the cyclotron frequency such a circumstance is expected for moderate-β plasmas because of field depression by plasma diamagnetism. In Fig. 3(b) we have plotted the frequency shift as a function of the product of mean ion energy and line densi-

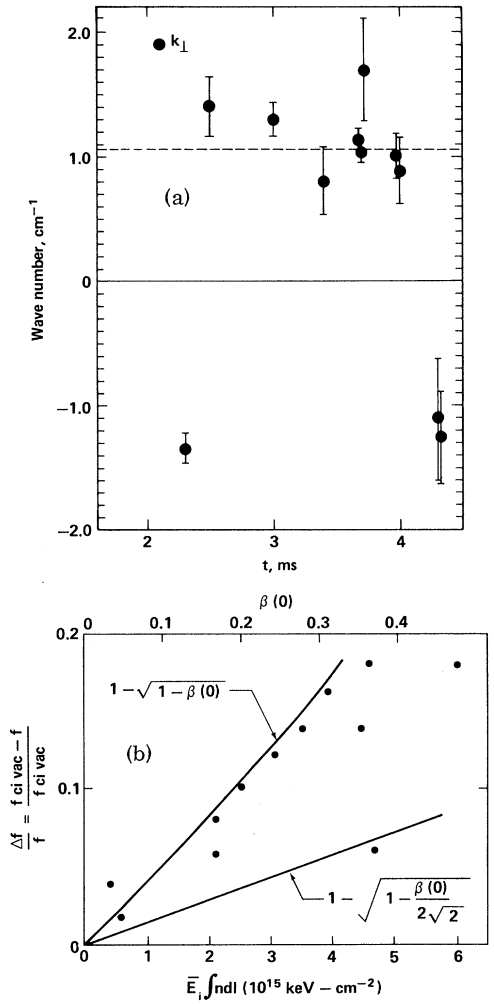

FIG. 3. (a) Wave numbers vs time of measurement. Dashed line is condition $\omega_i^* = \omega_{ci}$. (b) Frequency shift $\Delta f = f - f_{ci\ \mathrm{vac}}$ of measured frequency from vacuum ion-cyclotron frequency vs $\bar{E}_i \int n\,dl$ and center plasma beta, $\beta(0)$.

ty measured through the plasma center. β at the plasma center is related to $\bar{E}_i \int n\,dl$ by

$$\beta(0) = 8\pi \frac{n(0)\bar{E}_i}{B_{\mathrm{vac}}^2} = \frac{8\pi}{(\sqrt{\pi})R_{\mathrm{plasma}}} \frac{\bar{E}_i \int n\,dl}{B_{\mathrm{vac}}},$$

where $n(0) = \int n\,dl/\sqrt{\pi}R_p$ for the measured Gaussian line density profiles.

Also plotted in Fig. 3(b) are two curves corresponding to the frequency shift expected in the long, thin plasma approximation $\Delta f/f_0 = 1 - (1 - \beta)^{1/2}$. The upper curve is calculated for the center-plasma β and the lower curve for the density-weighted mean plasma β, $\bar{\beta}(0)/2\sqrt{2}$. Since the observed frequency shifts fall close to the $\beta(0)$ expectation, the data suggest that the oscilla-

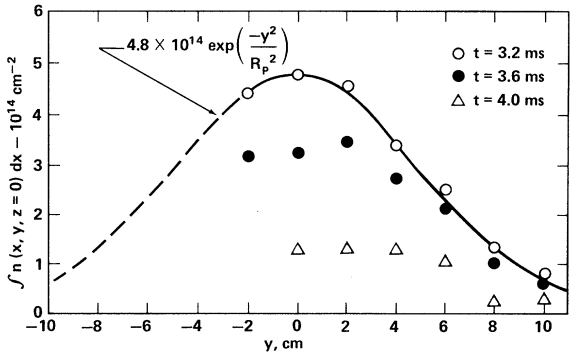

FIG. 4. Line density profiles in the vertical plasma midplane. Smooth curve is a Gaussian profile $\exp(-y^2/R_p^2)$ with mean plasma radius $R_p = 7$ cm.

tions are related to the center density rather than the density further out on the plasma profile where the radial density gradient is steeper. A related phenomenon is observed in Fig. 4 where we have plotted the radial line-density profile following onset of the decay. The profiles are obtained by measuring neutral beam attenuation along chords at the plasma midplane. The density decay is observed initially at the plasma center and then moves radially outward.

In connection with the above data we have performed a marginal stability analysis of the DCLC dispersion relation. The details of the calculation are available on request from one of us (W.C.T.). For the plasma parameters reported here, the predicted $k_\perp$ is ~ 30% below the condition obtained by equating the ion diamagnetic drift frequency $\omega^* = k_\perp c\bar{E}_i eBR_{\mathrm{plasma}}$ to the ion-cyclotron frequency, and the wave propagates in the direction of the ion diamagnetic drift.

In conclusion, we have measured the frequency and wavelength of electrostatic ion cyclotron oscillations in a stream stabilized mirror machine. A narrow-band ($\Delta f/f < 0.02$), single-mode spectrum near the ion cyclotron frequency is observed. For most of the plasma buildup and decay the wave propagates in the ion diamagnetic drift direction with $2.9 < k_\perp a_i < 6.1$. When the stabilizing stream plasma is shut off, the plasma loss rate increases, and there is a simultaneous increase of oscillation amplitude and ion heating although the wave spectral properties do not change. These observations support the wave-particle saturation of the DCLC mode proposed to explain the stability of mirror machines.[3] Early and late in the time evolution of the experiment the ion-cyclotron wave propagates opposite to the ion diamagnetic drift and this has not been ex-

plained by the DCLC dispersion relation.

This research was supported by the U. S. Energy Research and Development Administration under Contract No. W-7405-Eng-48.

[a]Permanent address: University of Texas, Austin, Tex. 78712.

[1]M. S. Ioffe, B. I. Kanaev, V. P. Pastukhov, and E. E. Yushmanov, Zh. Eksp. Teor. Fiz. 67, 2145 (1974) [Sov. Phys. JETP 40, 1064 (1975)].

[2]F. H. Coensgen *et al.*, Phys. Rev. Lett. 35, 1501 (1975).

[3]D. E. Baldwin, H. L. Berk, and L. D. Pearlstein, Phys. Rev. Lett. 36, 1051 (1976).

[4]R. F. Post and M. N. Rosenbluth, Phys. Fluids 9, 730 (1966).

[5]F. H. Coensgen *et al.*, Phys. Rev. Lett. 37, 143 (1976).

[6]W. E. Nexsen *et al.*, Bull. Am. Phys. Soc. 20, 1232 (1975).

[7]E. J. Powers and T. C. Simonen, J. Appl. Phys. 47, 3911 (1976).

[8]D. Smith and E. J. Powers, IEEE Trans. Plasma Sci. 2, 261 (1974).

[9]T. C. Simonen, Phys. Fluids 19, 1365 (1976).

Vacancy-Induced Ferromagnetism: The Registered Phase of ^{3}He on Grafoil

R. A. Guyer

Department of Physics and Astronomy, University of Massachusetts, Amherst, Massachusetts 01003

(Received 24 June 1977)

Submonolayer ^{3}He on Grafoil at density n just below the density of the registered phase, n_c, corresponds to a low-density solid with vacancy concentration $(n_c - n)/n_c$. Under suitable circumstances, these vacancies cause the solid to undergo a ferromagnetic transition.

During the past few years the submonolayer ^{3}He and ^{4}He systems on Grafoil have been the subject of intense experimental and theoretical investigation.[1] Analysis of the thermodynamic data on these systems shows the phase diagram of submonolayer helium (on Grafoil[2]) to be very similar to the phase diagram of bulk helium.[3,4] Recent NMR measurements of Richards and co-workers[5,6] on ^{3}He over much of the submonolayer phase diagram show this system to be described by particle motions qualitatively similar to those observed in bulk helium. In most regards the submonolayer helium systems (on Grafoil) are strikingly similar to the corresponding bulk helium systems. But, the two-dimensional (2D) helium systems reside in the periodic hexagonal potential wells of the Grafoil substrate. At certain coverages of the substrate, this potential coaxes the helium into the registered phase or "lattice-gas" phase.[3] The registered phase is an artificially low-density solid phase; it is the unique feature of the 2D helium phase diagram. This Letter describes a speculation about the nature of the low-temperature magnetic state of the registered phase of ^{3}He. The essential content of this speculation is that the registered phase can be formed with a reasonable concentration of ground-state vacancies *and* that these induce a ferromagnetic phase transition at $T \lesssim 5$ mK.

The onset of the registered phase is signaled by a λ-like signature in specific-heat data at about 3 K. In T_1 data, at constant temperature below T_c, the registered phase is seen as an asymmetric dip in T_1, as a function of coverage.[6] At fixed coverage, near the critical coverage n_c for the registered phase, T_1 decays rapidly as the temperature is lowered below T_c. The transition to the registered phase in ^{3}He is at $n_c = 0.0643$ part/Å^2 and $T_c = 2.03$ K. Strong vestiges of the registered phase are seen at coverages $|n - n_c|/n_c \lesssim 0.05$ on either side of n_c at temperatures of order T_c. Thus, the registered phase is a needle on the phase diagram, Fig. 1. At n_c the number of ^{3}He atoms on the Grafoil surface is $\frac{1}{3}$ of the number of binding sites on the surface. The atoms are localized near every third lattice site (they are in registry with one of three equivalent sublattices) at 4.20 Å from their nearest neighbors, Fig. 1(b). A solid, which is the monolayer analog of the bulk solid, is present on the phase diagram[7] at $0.078 \lesssim n \lesssim 0.110$; it "melts" at $n \approx 0.700$ so that the registered phase is a low-density island of solid surrounded by the liquid phase.[8]

Evidence for the localization and spin disorder of the registered phase comes from a variety of sources. (a) The entropy of ^{3}He and ^{4}He, calculated from specific-heat data at $T \geq 0.040$ K, dif-